Meteoritics & Planetary Science 40, Nr 2, 225–238 (2005)
Abstract available online at http://meteoritics.org

Chondrules in Antarctic micrometeorites

M. J. GENGE[1*], A. GILESKI[2], and M. M. GRADY[2]

[1]Department of Earth Science and Engineering, Imperial College London, Exhibition Road, London SW7 2AZ, UK
[2]Department of Mineralogy, The Natural History Museum, London SW7 5BD, UK
[*]Corresponding author. E-mail: m.genge@imperial.ac.uk

(Received 17 December 2003; revision accepted 20 October 2004)

Abstract–Previous studies of unmelted micrometeorites (>50 µm) recovered from Antarctic ice have concluded that chondrules, which are a major component of chondritic meteorites, are extremely rare among micrometeorites. We report the discovery of eight micrometeorites containing chondritic igneous objects, which strongly suggests that at least a portion of coarse-grained crystalline micrometeorites represent chondrule fragments. Six of the particles are identified as composite micrometeorites that contain chondritic igneous objects and fine-grained matrix. These particles suggest that at least some coarse-grained micrometeorites (cgMMs) may be derived from the same parent bodies as fine-grained micrometeorites. The new evidence indicates that, contrary to previous suggestions, the parent bodies of micrometeorites broadly resemble the parent asteroids of chondrule-bearing carbonaceous chondrites.

INTRODUCTION

Micrometeorites (MMs) are the fraction of extraterrestrial dust received by the Earth that survives atmospheric entry and is recovered from the surface of the Earth. Large numbers of these particles have been collected by melting and filtering of Antarctic ice (Maurette et al. 1991) and provide important samples of small bodies in the solar system.

Previous studies of Antarctic MMs have revealed the presence of particles that are unmelted and fine-grained, known as fine-grained MMs (fgMMs) (Fig. 1a), These particles have close compositional, textural, and mineralogical affinities to the matrices of CM2, CR2, and CI1 carbonaceous chondrites, suggesting that these particles originate as dust-sized debris from main belt asteroids (Kurat et al. 1994; Genge et al. 1997; Engrand et al. 1998). Chondrules, which are abundant in CM2 chondrites (up to 15% by volume; Brearley et al. 1998) and CR2 chondrites (up to 50% by volume; Grossman et al. 1988), have only rarely been recognized among MMs (Kurat et al. 1996). The rarity of chondrules among MMs has been cited as evidence that the sampled parent bodies of MMs are distinct from those of known meteorite groups and might even be cometary rather than asteroidal in origin (Engrand et al. 1998).

Chondritic igneous particles are, nevertheless, present among MMs that might represent fragments of chondrules. These particles are known as coarse-grained MMs (cgMMs) (Genge et al. 1997) and are dominated by olivine and/or pyroxene and glass (Fig. 1b). Coarse-grained MMs are relatively abundant but have not been considered fragments of chondrules because they generally lack evidence for the sub-spherical morphologies of these objects (Kurat et al. 1996; Engrand et al. 1998).

Whether samples of chondrules are present among Antarctic MMs is an important question, as it has significant implications for the sources of MMs within the solar system. If chondrule samples are exceedingly rare among MMs, as suggested by Engrand et al. (1998), then MMs necessarily sample parent bodies distinct from all carbonaceous chondrite groups except the CI1 chondrites. There could be three possible explanations for this difference: 1) MMs are a highly biased sample of main belt asteroids, derived from a few sources that are distinct from the parent bodies of meteorites, 2) meteorites are a highly biased sample of main belt asteroids and the majority of these bodies do not contain chondrules, or 3) the majority of MMs are cometary materials.

In the present study, we report the discovery of eight MMs that include igneous objects that strongly resemble chondrules or chondrule fragments in their mineralogies, textures, compositions, and occurrences. This discovery indicates that chondrules are present within MM parent bodies and, by inference, suggests that many coarse-grained igneous MMs, which closely resemble the reported igneous objects, may likewise be chondrule fragments. The presence of fine-grained matrix and igneous objects within six of the

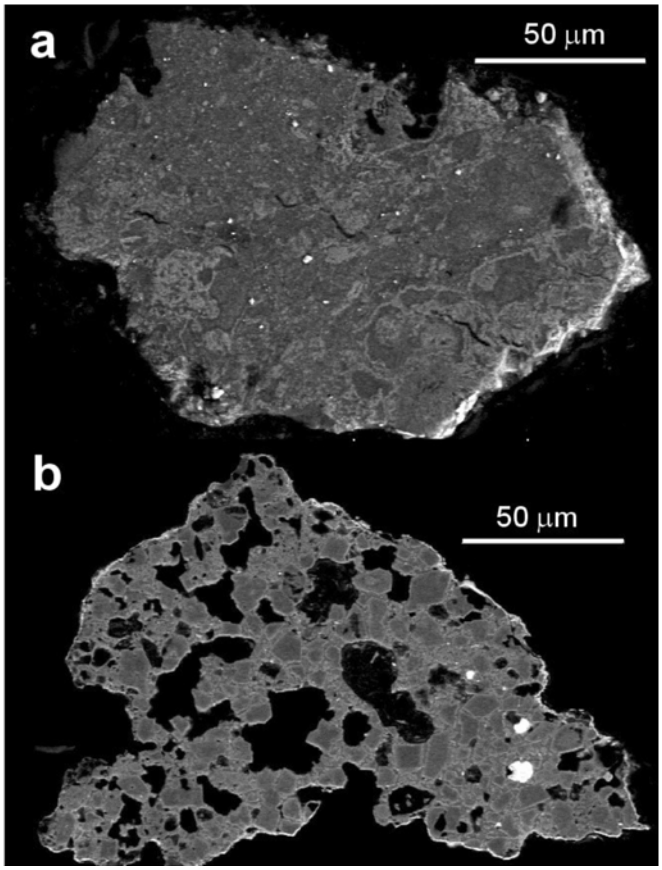

Fig. 1. Backscattered electron images of representative a) fine-grained MMs and b) coarse-grained MMs. Fine-grained MMs are dominated by submicron ferromagnesian silicates that represent phyllosilicates or the dehydration products. Coarse-grained MMs are dominated by anhydrous silicates, glass, and sometimes metal and/or sulfides. Most cgMMs have igneous textures.

eight particles furthermore suggests that fine-grained, carbonaceous chondrite-like MMs and coarse-grained MMs can be derived from the same parent asteroids. The realization that chondrule fragments are present among MMs indicates that the parent bodies of these materials have affinities to those of CM2 and CR2 carbonaceous chondrites and are likely to be derived from primitive asteroids.

SAMPLES AND TECHNIQUES

The eight MMs reported in the current work were all collected by melting and filtering Antarctic ice. Seven of the particles were recovered by melting and filtering of blue ice near Cap Prudhomme by Maurette and co-workers in 1994 (e.g., Maurette et al. 1991) and particle SP96-100-001 was recovered from the South Pole water well by Taylor and Harvey in 1996 (e.g., Taylor et al. 2000). The eight particles described in the current paper were discovered among a total of 310 unmelted MMs derived mainly from Cap Prudhomme. The selection procedures used to separate and prepare samples as polished grain mounts are described in detail in Genge et al. (1997).

Backscattered electron images (BEI) of the particles described in the current work were obtained using a JEOL 5900LV scanning electron microscope at the Natural History Museum. Analyses of minerals and mesostasis were determined by energy dispersive spectroscopy using the JEOL 5900LV. Analyses were obtained using a beam current of 1 nA at 20 kV and standard matrix corrections applied with a gain calibration on a vanadium standard. Repeat analyses of mineral standards suggest detection limits of about 0.2 to 0.5 wt% for most elements heavier than fluorine. Accuracy and precision vary by element, but are of a similar order of magnitude as detection limits (<1 wt%).

Wavelength dispersive spectroscopy was used to determine the compositions of minerals larger than about 4 μm in diameter and to obtain spot analyses of fine-grained materials present within the particles. The analyses were obtained using a Cameca SX50 at the Natural History Museum. Analyses were obtained against mineral standards and Cameca matrix corrections were applied. Repeat analyses of mineral standards suggest detection limits of 0.05 wt% or less for most elements. Accuracy and precision vary by element, but are of a similar order of magnitude as detection limits (<0.1 wt%).

Results

Six of the eight reported MMs are composite particles containing both fine-grained matrix and coarse-grained igneous objects; two particles (166 and 105) consist entirely of igneous material and are thus cgMMs. The igneous objects found in these particles are dominated by olivine, pyroxene, and glassy mesostasis and, like chondrules, are broadly chondritic in bulk composition. The textures and mineralogies of the igneous objects differ from particle to particle, but are consistent with formation by the rapid cooling of chondritic liquids. Mineral compositions from the MMs are summarized in Table 1.

Mineralogy and Texture of Igneous Objects

The igneous objects within the reported MMs can be subdivided into three groups on the basis of their mineralogical and textural properties: 1) reduced objects with Mg-rich silicates, 2) oxidized objects with Fe-bearing silicates, and 3) radiating pyroxene (RP) objects.

Four of the MMs (particles 164, 311, 320, and 329) contain reduced igneous objects that are dominated by subhedral to euhedral enstatite phenocrysts (Fs_{2-8}) with small interstitial areas of calcium-aluminum-rich, ferromagnesian glass (Fig. 2). Sub-spherical Fe-rich droplets (<5 μm in diameter) occur in all particles (except particle 320) and consist of FeNi-bearing metal or oxide (0.5–5.6 wt% Ni). In

Table 1. The compositions of phases within ITOs in wt%.[a] Analyses labeled with * were obtained by EMPA, the remaining analyses by EDS.

Sample	164*	164*[b]	001*	001*	001	1661	3111	329	329	320
Phase	Px	Mes	Px	Ol	Mes	Px	Px	Px	Mes	Px
Na_2O	b.d.	0.55	b.d.	b.d.	0.9	b.d.	b.d.	b.d.	1.3	b.d.
FeO	2.78	19.24	11.20	18.06	22.9	2.8	2.4	b.d.	18.1	3.5
CaO	0.70	3.74	1.44	0.29	9.9	2.9	0.6	2.2	6.7	b.d.
SiO_2	56.27	41.21	51.61	38.49	50.0	52.1	56.2	57.7	47.6	56.6
MgO	38.37	23.32	31.52	42.38	7.5	37.1	36.7	37.7	20.8	37.2
Al_2O_3	1.05	8.65	0.97	0.10	9.0	3.2	1.1	1.7	5.2	1.0
MnO	b.d.	0.38	0.43	0.67	0.4	b.d.	b.d.	b.d.	0.4	b.d.
Cr_2O_3	0.19	1.17	0.81	0.35	0.3	0.9	0.65	0.6	0.8	1.3
Totals	100.23	98.34	98.27	100.45	98.0	99.4	97.99	100.5	101.2	100.0

[a]K, S, Ti, Ni, and P were below detection limits in all analyses.
[b]Analyses affected by matrix overlap with mesostasis.

particle 164, the FeNi oxides are interconnected by thin veins filled with similar materials (Fig. 2a). The oxides in these particles have stoichiometric close to magnetite (Fe_3O_4), but contain accessory Si, Ni, P, and S. In places, small patches of relict FeNi metal (<5.6 wt% Ni) occur within the oxides, suggesting that these were metal droplets altered to ferrihydrite by aqueous alteration. Dirty magnetites containing Si and P are commonly observed in Antarctic MMs; previous studies have shown that this material consists primarily of ferrihydrite (Engrand et al. 1999; Engrand et al. 1998; Genge et al. 2001). Engrand et al. (1999) have argued that such ferrihydrite-dominated oxide assemblages (known as COPS) are extraterrestrial, based on their high D/H ratios. In contrast, Genge et al. (2001) suggest that these are formed by terrestrial alteration, based on their low decomposition temperatures and occurrence in MMs. All four particles have a partial magnetite rim about 2 μm thick, which is typical of MMs and is thought to form during atmospheric entry heating (Kurat et al. 1994; Toppani et al. 2003).

The igneous object in particle 001 also has a porphyritic texture, but contains Fe-rich anhydrous silicates and no metal or oxide droplets (Fig. 3). The object contains both olivine (Fa_{19}) and low-Ca pyroxene ($Fs_{13–16}$) phenocrysts with some of the olivines partially enclosed within the pyroxene (Fig. 3b). Thin (<4 μm) overgrowths of more iron-rich olivine (<Fa_{50}) are present on the olivine phenocrysts and give them a euhedral morphology. Small fayalitic olivine microphenocrysts also occur in the calcium-aluminum-rich glassy mesostasis and are concentrated close to the external surface of the particle, where they grade into a vesicular rim consisting entirely of zoned fayalitic olivine (~Fa_{50}), microphenocrysts (<4 μm in diameter), and interstitial glass. This microporphyritic rim surrounds the entire particle, including the fine-grained portion (Figs. 3b and 3c), and is typical of the melted rims formed during atmospheric entry that are common on other MMs (Genge et al. 1997).

Micrometeorites 310, 166, and 105 have igneous objects dominated by thin (<5 μm wide) pyroxene dendrites with interstitial glass. Particle 310 also contains small (<0.5 μm) spherical, iron-rich grains within the glass mesostasis, which are probably metal droplets (Figs. 4e and 4f). In these particles, the pyroxene dendrites have a radiating arrangement. Due to their small size, the pyroxene dendrites are difficult to analyze quantitatively. However, repeat analyses suggest compositions of ~Fs_{19}, Fs_{20}, and ~Fs_4 in particles 310, 105, and 166, respectively, with a mesostasis that is rich in Ca and Al. Particles 166 and 105 lack fine-grained matrix portions (Figs. 4a–d), but particle 166 has a vesicular igneous rim consisting of fayalitic olivine microphenocrysts and magnetite within interstitial glass (Fig. 4b). The rim completely surrounds the particle.

The igneous objects in all the studied particles contain subrounded voids in the mesostasis of particles and often glass remains only as small interstitial areas trapped between phenocrysts and the vesicles. Subrounded voids are also present within some of the anhydrous silicates and submicron voids are present within the mesostasis of the radiating pyroxene igneous objects between the dendrites (e.g., Figs. 2b and 2d). The majority of these voids are interpreted here as vesicles on the basis of their smooth surfaces, spherical or elliptical morphologies, and occurrence largely within the mesostasis of particles. However, some irregularly shaped voids located on the surface of the MMs (for example, in particle 164 [Fig. 2a]) may represent etching pits due to submersion in water and preferential dissolution of glass (Harvey, personal communication).

Fine-Grained Matrix

Six of the studied MMs have chondritic fine-grained matrix and are thus composite particles intermediate between the more common fine-grained and coarse-grained MMs. Particles 164 and 310 have only small amounts of fine-grained matrix present at the margins of their component igneous objects (Figs. 2a and 4e), whereas the other composite particles have more substantial fine-grained areas. Particles 311 and 329 are surrounded by complete rims of fine-grained matrix (Figs. 2b and 2d) and in particles 001 and

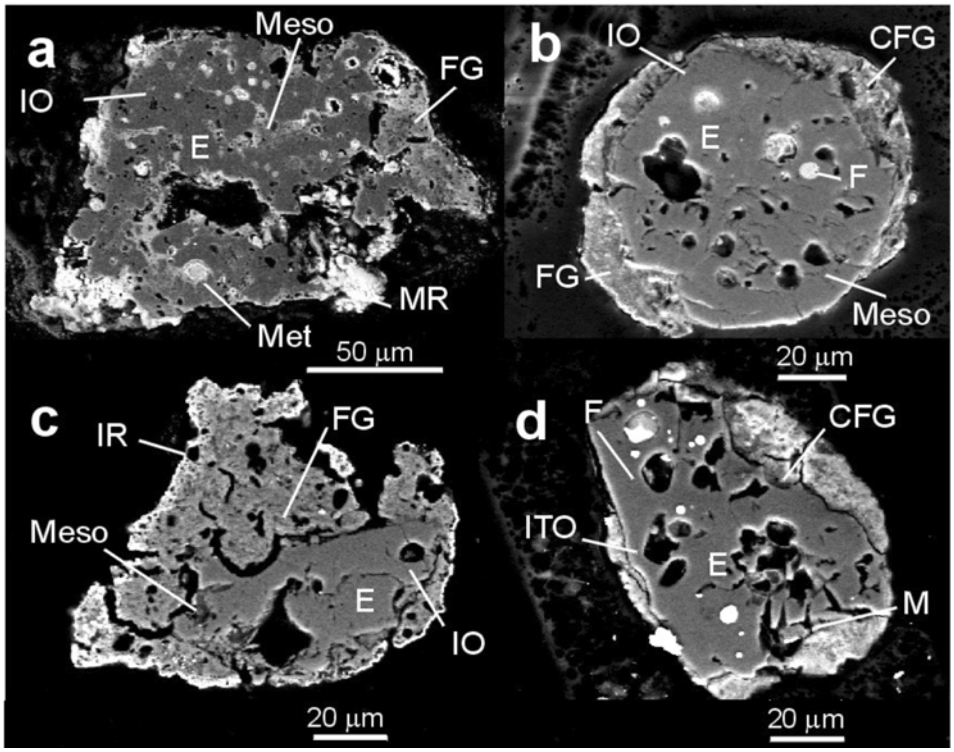

Fig. 2. Backscattered electron images of the four enstatite-bearing composite MMs: a) CP94-100-164; b) CP94-50-311; c) CP94-50-320; d) CP94-50-329. IO = igneous object; FG = fine-grained matrix; CFG = matrix containing coarse 'phyllosilicate-like' phases; E = enstatite; M = mesostasis; F = iron-nickel metal; IR = igneous rim; MR = magnetite rim.

320, the matrix comprises approximately 70% of the particles by volume (Figs. 3a and 2c, respectively).

Average electron microprobe analyses of the fine-grained matrices reveal that they have broadly chondritic compositions (Figs. 5 and 6). Comparison of elemental ratios to Si for 12 major and minor elements indicate the fine-grained matrix of these particles has a close affinity to those of fine-grained MMs, which are themselves closely similar to the matrix compositions of CM2 and CR2 chondrites (Genge et al. 1997). Divergences from CM2 and CR2 matrix include depletions in Ni, Ca, and S that are commonly observed in all fine-grained MMs and are probably the result of alteration in the terrestrial environment or entry heating. The compositions of the fine-grained matrices from the reported composite MMs fall mainly within the range of fine-grained MMs (Genge et al. 1997) to within analytical uncertainties (Fig. 6).

High-magnification BEI reveal the presence of abundant submicron acicular to sheet-like phases within the fine-grained matrices of these particles. In previous studies, such acicular grains have been suggested to be phyllosilicates or their thermal decomposition products, the dehydroxylates (e.g., Genge et al. 1997; Genge et al. 2001). Phyllosilicates have, however, only rarely been observed in high-resolution transmission electron microscopy (TEM) investigations of ultramicrotomed thin sections of MMs and most 'unaltered' fine-grained particles are dominated by elongate acicular to sheet-like amorphous ferromagnesian silicates that are thought to be dehydroxylates after serpentine or smectite (Genge et al. 1997; Genge et al. 2001; Nakamura et al. 2001, 2002). The microtexture of the matrices of the current particles is identical to that of other fgMMs and therefore probably represents hydrated matrix that has been heated to temperatures greater than 600 °C during atmospheric entry such that the phyllosilicates have dehydrated (Greshake et al. 1998; Toppani et al. 2001).

The textures of the fine-grained matrices, although broadly similar to each other and to fgMMs, exhibit some variability. Particles 164, 310, and 320 all have compact low-porosity matrices dominated by submicron acicular silicates (Figs. 2a, 4e, and 2c), whereas particle 311 has a two-component matrix in which one portion is dominated by much coarser acicular phases (<5 µm) and the other is much finer-grained and contains dispersed submicron iron oxide phases (Fig. 2b). Both areas, however, have similar chondritic compositions. The matrix attached to particle 329 also consists of relatively coarse acicular phases (Fig. 2d). In general, the matrices of the above five particles are similar in texture to both fgMMs (Genge et al. 1997) and the matrices of CI1, CM2, and CR2 chondrites.

The matrix in particle 001 is considerably more porous than in the other particles (~50% by volume) and is dominated by micron-sized subhedral to euhedral olivines and pyroxenes contained in a network of fluffy acicular to sheet-like phases (Fig. 3a). Isolated anhedral olivines and pyroxenes (<10 μm in size) also occur embedded in the matrix and are probably fragments of larger grains. A single silica grain 5 μm in length is also present and is surrounded by a reaction rim of fayalitic olivine. The origin of this grain will not be considered in the current work. The high porosity of this matrix and the presence of micron-sized, relatively Mg-rich anhydrous silicates is distinctly different from that of the matrices of known carbonaceous chondrites. Although its composition is similar to that of CM2 chondrite matrix, its high porosity and the abundance of matrix olivines and pyroxenes suggest it has experienced less aqueous alteration than CM2 chondrites. Similar highly porous fgMMs, dominated by olivine and pyroxenes, have been recognized (Genge et al. 1997).

One feature of the matrices of the reported particles that is distinct from meteorite matrix is the presence of subspherical or rounded voids that are much larger than pore spaces. The shapes of these voids suggest that they are vesicles arising from degassing of volatile components in the matrix during entry heating and are thus similar to those present within other fgMMs (Genge et al. 1997).

External Morphology of the Igneous Objects

The boundaries between the igneous objects and the fine-grained matrices in composite particles are irregular and truncate phenocrysts, which clearly identifies them as fragments of larger igneous objects. All radiating pyroxene igneous objects (166, 105, and 310; Fig. 4), however, have outer surfaces (or boundaries with fine-grained matrix) that are smooth convex curves. In particles 166 and 105, the surface is evidently part of an original subspherical outline cut by fracture surfaces.

DISCUSSION

On the basis of their textural, mineralogical, and morphological properties, as discussed below, the MMs reported here are suggested to be fragments of chondrules derived from primitive chondritic asteroids. Furthermore, the close similarity between the igneous portions of the reported composite MMs and cgMMs also suggests that the majority of cgMMs may likewise represent chondrule fragments. A detailed comparison of cgMMs, igneous objects within composite MMs, and chondrules will be given in a further publication. The relationship between cgMMs in general and chondrules is thus tentative at present.

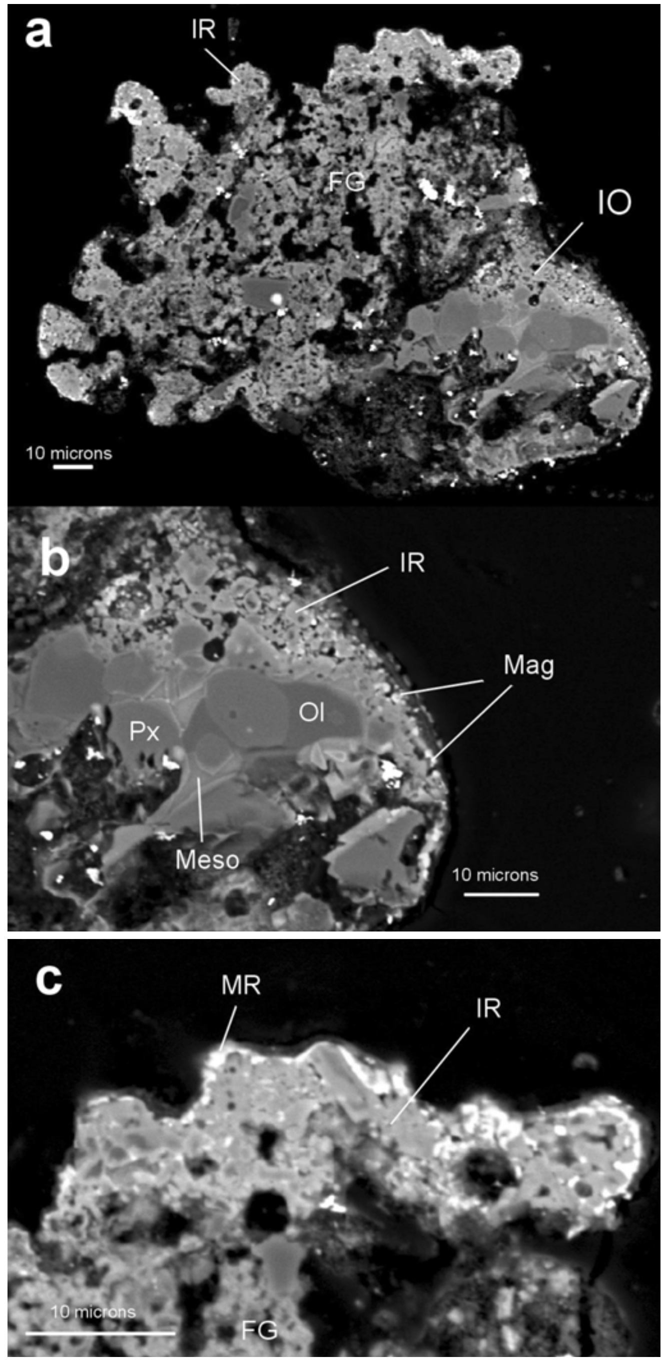

Fig. 3. Backscattered electron images of a) composite particle SP96-100-001; b) the exterior margin of the igneous object in this particle, showing the igneous rim consisting of fayalitic olivine. Magnetite grains are concentrated at the external edge of the igneous rim but do not form a continuous rim; c) a similar igneous rim consisting of fayalitic olivine microphenocrysts. Glass and magnetite also occur surrounding the fine-grained porous matrix of this particle. IO = igneous object; FG = fine-grained matrix; Px = pyroxene; M = glassy mesostasis; Ol = olivine; IR = igneous microporphyritic rim.

Textures and Mineral Assemblages

Three petrological-textural groups of igneous object are observed in the present study: 1) reduced, metal-bearing enstatite-dominated porphyritic objects, 2) oxidized, metal-free Fe-bearing silicate porphyritic objects, and 3) radiating pyroxene objects.

This distribution of groups strongly resembles that of

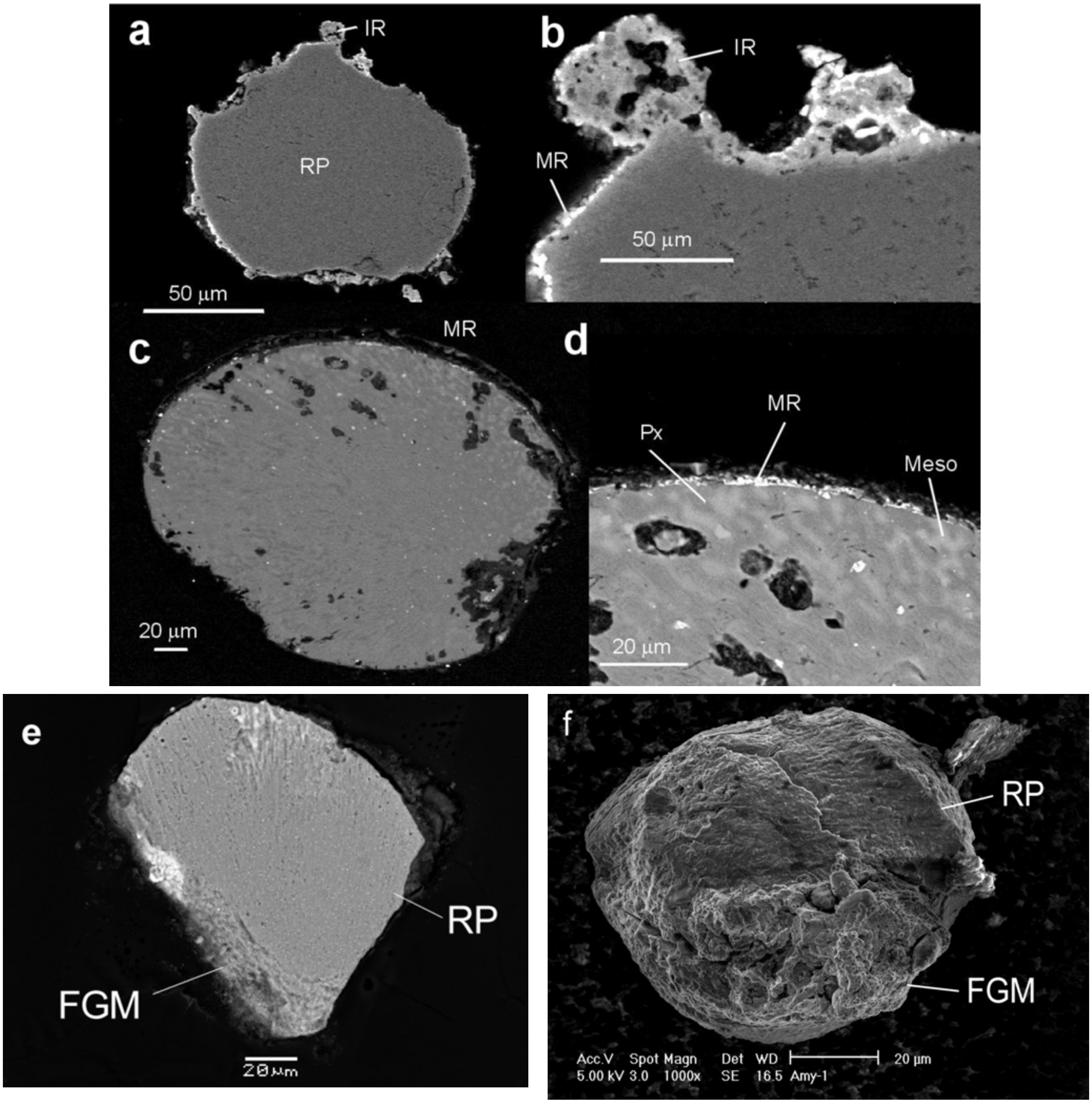

Fig. 4. Backscattered electron images of the three particles dominated by radiating pyroxene. a) Particle CP94-50-166 has a spherical morphology and is surrounded by b) a vesicular igneous rim consisting of zoned, fayalitic olivines and glass. Magnetite forms an exterior rim. c) Particle CP94-100-105 has a spheroidal shape and exhibits d) an external magnetite rim. Irregular voids in this particle are probably due to etching by exposure to water in the Antarctic. e) Particle CP94-100-310 that has a selvage of fine-grained matrix along its right side. The backscattered electron contrast between the fine-grained matrix and the radiating pyroxene igneous object is very low; however, the matrix can be distinguished from its moderate porosity and distinct composition. f) The small selvage of porous fine-grained matrix can be better distinguished from the RP igneous object in this secondary electron image of the particle exterior. RP = radiating pyroxene with interstitial glass; IR = igneous microporphyritic rim; MR = magnetite rim; FGM = fine-grained matrix.

type I(B), type II(AB), and radiating pyroxene chondrules, respectively (e.g., Brearley et al. 1998), although barred olivine textures, similar to barred olivine chondrules, are not observed. The absence of barred olivine textures is problematic, but will not be discussed further here since the reported eight particles (out of a total of 469 MMs) do not represent a statistically significant sample to examine the relative abundance of textural types. Ignoring the effects of alteration in the terrestrial environment (discussed below), the mineral assemblages and textures of the igneous objects observed here are indistinguishable from those of chondrules.

Atmospheric Heating Effects

Several features of the reported MMs have occurrences that suggest they are the result of atmospheric entry heating and are not original features of the particles. Microporphyritic vesicular rims dominated by Fe-rich zoned olivines observed on particles 166 and 001 that extend over the entire external surfaces of these particles are identical to igneous rims observed on other non-composite fgMM and cgMMs (Genge et al. 1997; Genge et al. 2004). The surface correlated nature of such rims and their discordant relationship with large unmelted mineral grains within the cores of MMs indicates that these originate by surface melting during atmospheric entry heating (Toppani et al. 2001).

That the microporphyritic rims observed on particles 166 and 001 formed due to surface melting during atmospheric entry is significant because it clearly indicates that the igneous objects within these objects are primary features derived from the parent body rather than being formed by heterogeneous melting during entry heating. Within the composite particles, the primary nature of the igneous objects is suggested by their interfaces with the adjacent fine-grained matrix that are, in most cases, irregular fracture surfaces.

Particles 166 and 105 have subspherical particle shapes and radiating textures, broadly resembling radiating olivine cosmic spherules. These spherules are formed by extensive melting of dust particles during atmospheric entry and are relatively abundant among MMs. The mineralogies of particles 166 and 105, however, differ from cosmic spherules as they are dominated by pyroxene rather than olivine. The crystallization of phenocrysts of pyroxene is kinetically impeded at the high cooling rates experienced by cosmic spherules (Taylor et al. 1991) and radiating pyroxene spherules are unknown among cosmic spherules. Pyroxene occurs very rarely within cosmic spherules as small, dendritic crystals within the glassy mesostasis of porphyritic olivine spherules (Genge unpublished data). Particle 166 also has a microporphyritic vesicular rim; both particles have outer magnetite rims. These are features not found on cosmic spherules (Genge et al. 1997) and indicate categorically that the igneous textures of these particles predate atmospheric entry despite their subspherical morphologies.

The presence of external magnetite rims on all the reported MMs indicates a pre-atmospheric origin for the observed igneous objects. Magnetite rims are observed on all MMs except the least heated and the most extensively melted; that is, the cosmic spherules (e.g., Genge et al. 1997; Toppani et al. 2001, 2003). The presence of magnetite rims on particles with spherical morphology, such as particle 166, is thus very strong evidence that these did not form as cosmic spherules during to atmospheric entry.

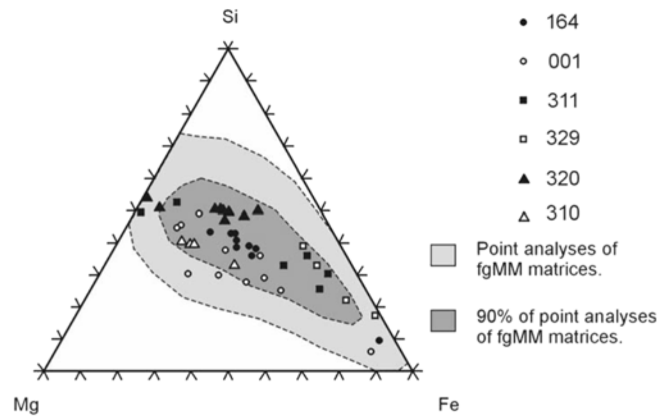

Fig. 5. Fe-Mg-Si abundance of the fine-grained matrices of the composite particles and fgMMs (Genge et al. 1997).

Another textural feature associated with the microporphyritic melted rim on particle 001 is the presence of zoned Fe-rich microphenocrysts in the mesostasis of the igneous object and overgrowths on its phenocrysts (Fig. 7). These grade into the rim and are evidently formed during entry heating. The presence of these crystals within the glassy mesostasis of this particle indicates diffusion and crystal growth in the mesostasis during reheating in the atmosphere and implies remelting of the glass. This might appear to be contrary to the survival of fine-grained matrix in this particle; however, remobilization of the glassy mesostasis will occur at its glass transition temperature, which is two-thirds of the equilibrium melting temperature of the glass (~1100 °C) and at lower temperatures than the solidus of fine-grained matrix (~1350 °C). It is important to understand that this process does not strictly represent melting. Glass is already a liquid and therefore cannot be melted. On heating through the glass transition, the viscosity of a glass decreases and diffusion rates become high enough to allow crystallization.

Remobilization of glass may also explain the presence of vesicles within the mesostases of the igneous objects through exsolution of volatiles contained in the mesostasis. In contrast to the igneous objects reported here, vesicles are rare in the mesostases of chondrules, even though they have finite volatile inventories. In the atmosphere, however, the reheating of chondrules occurs under higher oxygen fugacities than during chondrule formation and volatile elements such as C and S, which are dissolved in the mesostasis, might be expected to exsolve into the gas phase as CO_2 and SO_2 to generate vesicles.

Evidence that vesicles form in chondrule mesostases during atmospheric entry heating can be seen in the fusion crusts of chondritic meteorites since vesicles occur within chondrules in the heat affected, partially melted, substrate below the outer melted crust (Fig. 7; Genge et al. 1999).

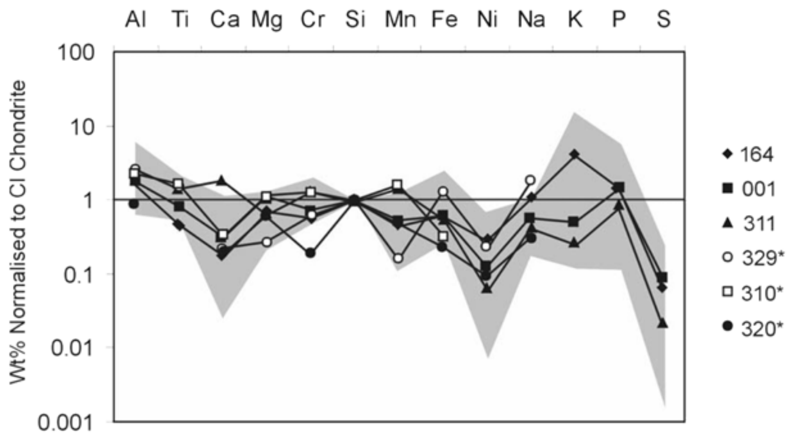

Fig. 6. Elemental ratios to Si, normalized to CI for the fine-grained matrices of composite particles compared with those of fine-grained MMs (Genge et al. 1997).

Vesicles in igneous objects reported here are therefore likely to form due to remobilization of glassy mesostasis, as it is heated above its glass transition temperature and degassing during entry heating. This also implies that the mesostases of the igneous objects contains broadly similar volatile inventories to chondrule mesostases.

Mineral and Mesostasis Compositions

Minor element compositions of anhydrous silicates within the igneous objects of the reported MMs (Table 1) are similar to those observed for chondrules of types I and II. The abundance of refractory elements (CaO, Al_2O_3, and TiO_2) and MnO, Cr_2O_3, and FeO in particular all fall within the range of these phases from chondrules within types 2 and 3 chondrites (Figs. 8a–g). Mineral minor and major element compositions of anhydrous silicates are not particularly diagnostic of specific chondritic meteorite groups (e.g., Brearley et al. 1998). The Mn content of olivines within particle 001, however, suggests an affinity with olivines from type 3 ordinary chondrites rather than carbonaceous chondrites.

Reliable analyses of the glassy mesostasis of the igneous objects are difficult to obtain due to their small sizes and matrix overlap with surrounding phases. However, the compositions of the mesostases in particles 001, 164, and 329 were determined (Table 1). The mesostases of particles 001 and 329 have CaO, Cr_2O_2, Na_2O, MnO, and SiO_2 within the range of most chondrules from type 2 and 3 chondrites (Figs. 8h–j). Al_2O_3 abundance in these particles, however, fall towards the minimum values relative to SiO_2 observed in chondrule matrices. The mesostasis of particle 164 exhibits Al_2O_3, CaO, and Na_2O significantly lower than that of chondrule mesostasis. Analyses of mesostasis within this particle, however, show significant variation which, together with the small size of mesostasis areas, suggests that the analyses are affected by significant matrix overlap with the surrounding enstatites. The analysis with the highest Na_2O, Al_2O_3, and CaO content is presented here as the most representative, yet these elements are likely to be present in greater abundance within the mesostasis glass.

The largest difference between chondrules and the reported igneous objects is in the FeO abundance of the mesostasis. FeO is higher (19–23 wt%) in the mesostases of the igneous objects within the MMs than in chondrules from type 2 or 3 chondrites (<17 wt%; Fig. 8h). However, metal and/or sulfide present in the mesostasis may have dissolved within the silicate glass during remobilization of the glass under relatively oxidizing conditions in the atmosphere, causing increases in the Fe content of the glass. This process is observed in fusion crusts where Fe enrichment of the silicate fusion crust melt occurs by reaction of FeNi metal with the melt under relatively oxidizing conditions during entry heating (Genge and Grady 1999). This process occurs in fusion crusts and their underlying thermally altered substrate at temperatures above and below the solidus. The iron enrichment of the mesostases of the igneous objects relative to chondrules can therefore probably be attributed to changes arising during entry heating.

Shape and Surface Morphology

Until the current work, only a single cgMM has been reported as a chondrule fragment; it was identified on the basis of the presence of a curved portion of its surface and its unfractionated rare earth element patterns, precluding an origin as a differentiated igneous particle (Kurat et al. 1996). An origin as chondrule fragments for other cgMMs has been dismissed because they lack smooth, curved surfaces.

Among the MMs reported in the current work, however, all three RP particles have smooth, curved surfaces, suggesting that these are chondrules or fragments of chondrules. As discussed above, the presence of radial pyroxenes within these objects categorically precludes an origin as cosmic spherules formed during atmospheric entry and strongly suggests that these are igneous objects that were present on the parent body.

Radiating pyroxene particles 166 and 105 are almost completely surrounded by a smooth, curved surface and thus appear to be nearly whole RP chondrules. The diameters of these objects are, however, smaller than the average chondrule sizes observed within chondrites (e.g., Grossman et al. 1988). Coarse-grained MMs, 50–100 µm in size, with radiating pyroxene textures are observed among micrometeorites lacking smooth, curved surfaces and are instead bounded by irregular fractures (Fig. 9). It is suggested here that such particles may represent internal fragments of larger RP chondrules. Particles 166 and 105 may therefore simply be small RP chondrules that are only readily recognized because they retain their smooth external surfaces.

The majority of the igneous objects within the MMs reported here lack smooth, curved external surfaces and instead exhibit irregular boundaries with fine-grained matrix. In most of the particles, these surfaces truncate phenocryst phases and are necessarily fracture surfaces. These igneous objects within composite particles must therefore be small fragments of larger chondritic igneous objects that were present on the parent body.

Most chondrules, however, are not smooth spheres, but have rounded, irregular surfaces on scales <50 µm (e.g., Grossman et al. 1988). Micrometeorites that sample chondrules, either as cgMMs or as igneous objects within composite particles, are therefore unlikely to exhibit smooth, curved surfaces, even if they do sample the external surface of a chondrule.

One exception may be radiating pyroxene objects. In chondrites radiating pyroxene chondrules commonly have spherical or ellipsoidal droplet shapes and relatively smooth surfaces. Because of this, small portions of the surfaces of fragmented RP chondrules may be identifiable. It is significant, then, that the only particles with smooth, curved, ‘chondrule-like’ surfaces also have radiating pyroxene textures (reported here [CP94-100-166, CP94-100-105] and in previous studies [Kurat et al. 1996]).

The absence of smooth, curved surfaces and spherical morphologies on the majority igneous objects reported here does not preclude an origin as samples of chondrules. The observation that chondrules in chondrites are rarely smooth, spherical objects implies that the external surfaces of chondrules will be difficult to recognize in small fragments of these objects. The observation in several of the particles that the boundary between the igneous object and fine-grained matrix is a fracture surface suggests that these particles were already chondrule fragments on the parent body.

The absence of whole non-RP chondrules among MMs is problematic. But observations of chondrites reveal that fragments of chondrules are very common are common (e.g., Grossman et al. 1988). Micrometeorites generated as dust-sized debris from such parent bodies will therefore be likely to sample chondrule fragments.

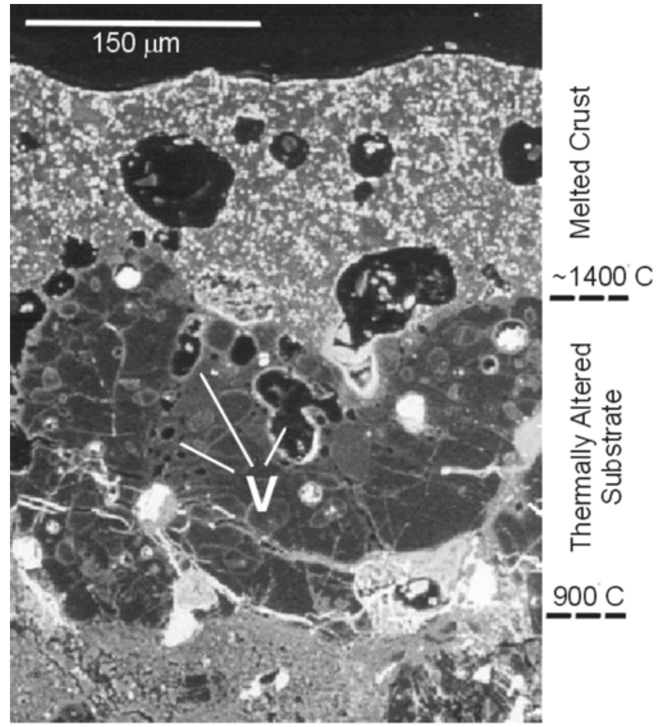

Fig. 7. Vesicles (V) formed in glassy chondrule mesostasis in the fusion crust of Lance (CO3) due to remobilization of glass in the thermally altered substrate below the outer melted crust. In this image, several large vesicles can be seen within the glassy mesostasis of the chondrule (Genge and Grady 1999). Vesicles are likely to form once mesostasis glass remobilizes. This will occur at temperatures about the glass transition temperature (roughly two-thirds the equilibrium melting temperature) when the glass becomes capable of flow due to decreases in viscosity.

Fragmentation of chondrules during dust production may also play an important role in reducing the number of whole chondrules liberated as ejecta to become MMs. The behavior of shock waves in heterogeneous media (Melosh 1996) may explain the preferential fragmentation of chondrules. Compact igneous materials such as chondrules have much higher shock impedances than porous chondrite matrix (carbonaceous or ordinary chondrite) and consequently particle and shock wave velocities are higher in chondrules than in matrix. Interfaces between materials with different shock impedance causes the refraction and reflection of shock waves that will influence the nature of the dust-sized debris produced in hypervelocity collisions. Reverberation of shock waves within chondrules from the interface with the matrix is likely to result in heterogeneous peak pressures inside the chondrules and lead to fragmentation. Experimental fragmentation of heterogeneous ‘conglomerate’ targets consisting of materials with contrasting shock impedance support this contention and demonstrate that compact grains are generally fragmented (Ernstson et al. 2001).

Notwithstanding the arguments presented above, the size of MMs examined is predominantly smaller than that of chondrules in any chondrite group, since only 151 out of the

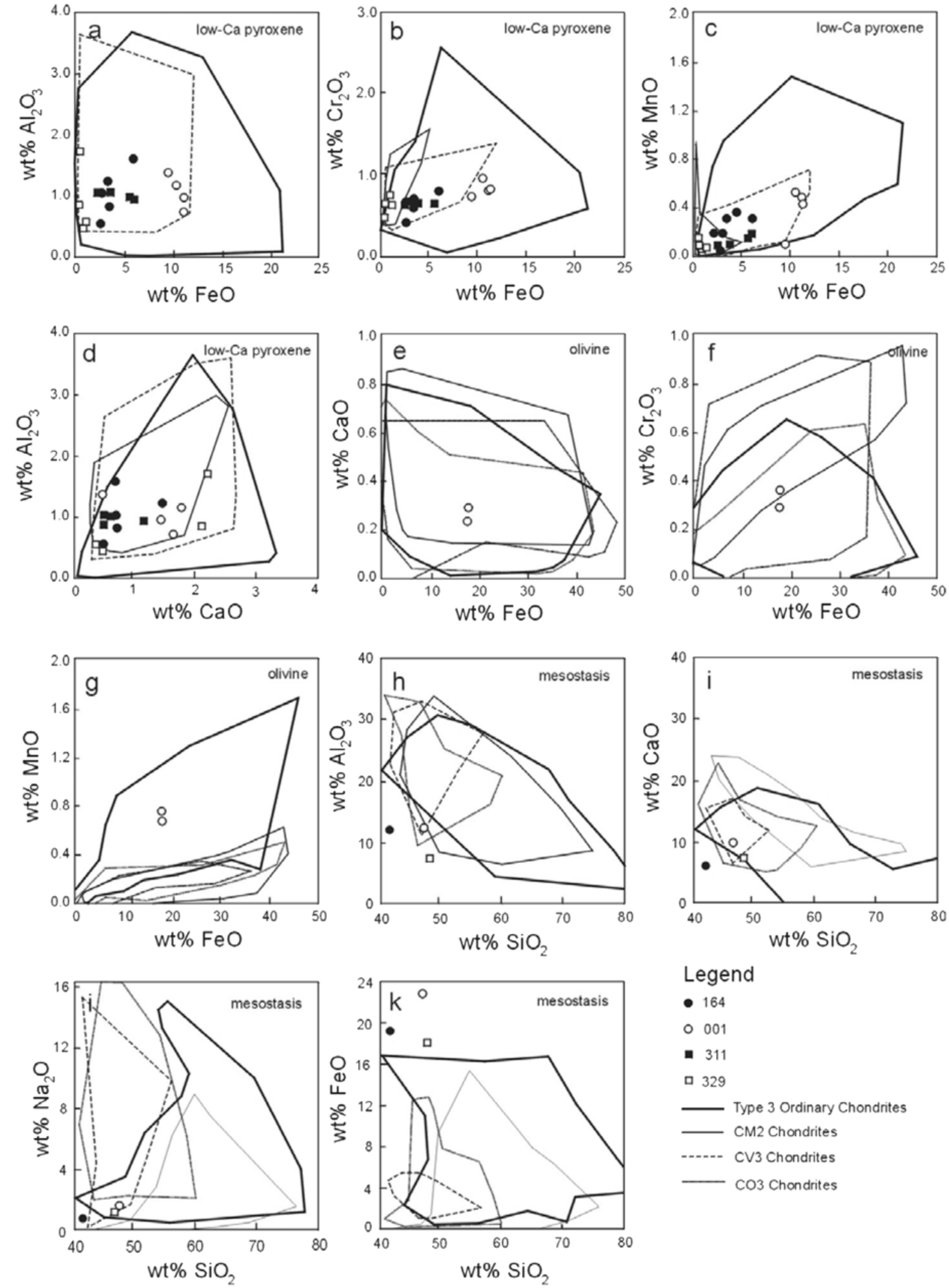

Fig. 8. The major and minor element compositions of phases from the reported igneous objects within the micrometeorites compared with the range of compositions of chondrule phases from a variety of chondrites: a–d) show the compositions of low-Ca pyroxenes; e–g) show the compositions of olivines in particle SP94-100-001; h–k) show the compositions of mesostases.

total 469 MMs were >100 µm. Most samples of whole chondrules would therefore be expected in the larger size ranges; too few of these particles were examined to provide a statistically robust estimate of their abundance.

Considering the relative size of chondrules and available MMs, the high abundance of chondrule fragments in chondrites, and their further fragmentation during the generation of micrometeoroids as impact ejecta, the rarity of whole chondrules among MMs is perhaps to be expected. The observation that those whole chondrules present among MMs are predominantly RP chondrules would therefore appear to be anomalous, but could relate to the relative size distributions of chondrule types in the parent bodies of MMs. A more statistically representative sample than presented in the current paper would be required to address this problem.

Fine-Grained Matrix

The fine-grained matrix observed in the six reported composite particles strongly resembles that of many fgMMs in both its composition and its texture. Particles with relatively coarse acicular phases similar to particle 311 are observed as fgMMs (Genge et al. 1997) and are similar to the textures of vugs of coarse-grained phyllosilicate observed in CI1 chondrites (Tomeoka et al. 1988).

Compact matrix similar to particles 310, 320, and 164 are observed in many fgMMs and are similar to those of CM2, CR2, and CI1 chondrites (Genge et al. 1997). The porous matrix of particle 001 differs considerably from that of the CM2, CR2, and CI1 chondrites, as it is dominated by relatively Mg-rich anhydrous silicates rather than phyllosilicate-like acicular to sheet-like minerals. Evidence for aqueous alteration is, however, present in the form of acicular phases comprising the interstitial materials that are probably dehydroxlates after phyllosilicate. Although differing from carbonaceous chondrite matrix, porous fine-grained MMs similar to particle 001 are relatively common among MMs (Genge et al. 2002).

Porous and compact fine-grained MMs often contain within their matrices isolated olivines and pyroxenes similar to those observed in particle 001, although this particle also contains an anomalous silica grain. Some isolated grains in the matrices of carbonaceous chondrites have been interpreted as primary nebula condensates (e.g., Klock et al. 1992). The discovery of chondrule fragments reported here suggests that isolated olivine and pyroxene in MMs could also be fragments of minerals from chondrules. In this study, however, such grains are not considered chondrule fragments since they lack igneous textures, nor are the particles containing them considered to be composite MMs.

In contrast to the aqueously altered fine-grained matrices of the reported MMs, no evidence for alteration is observed in the glassy mesostases of the igneous objects. Large differences in the degree of aqueous alteration are known in the CM2 chondrites, with meteorites such as Murchison containing many chondrules with pristine glassy mesostasis, whereas in meteorites such as Cold Bokkveld few unaltered chondrules remain. It has been suggested that altered chondrule materials do exist among MMs, but are generally classified as fine-grained matrix containing relict anhydrous silicates (Genge 2002). The absence of noticeable aqueous alteration of the igneous objects in the current particles is therefore no more surprising than the presence of pristine chondrules in CM2 or CR2 chondrites.

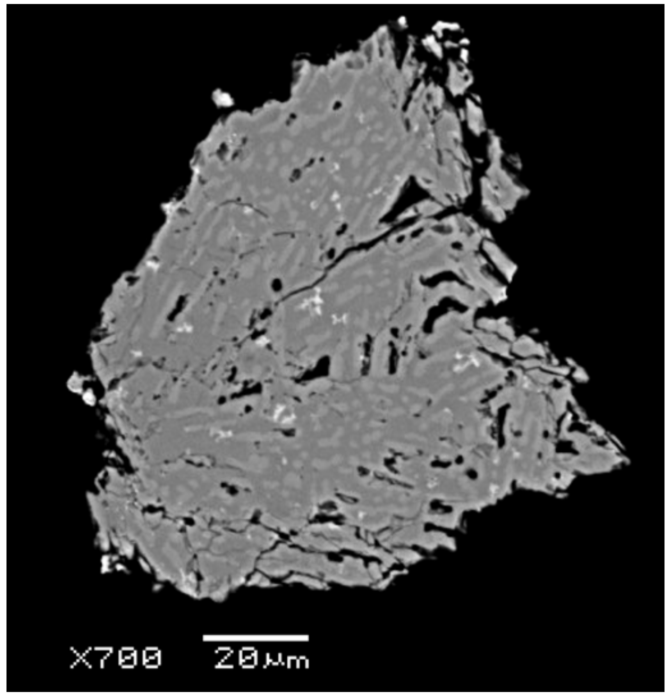

Fig. 9. A backscattered electron image of a radiating pyroxene cgMM (particle CP94-050-171) lacking a spherical outline.

Overall Evidence for Chondrule Fragments

The mineralogies, compositions, and textures of the seven MMs reported herein strongly suggest that they represent fragments of chondrules from the same set of asteroidal parent bodies as fgMMs and cgMMs. The arguments can be summarized as:

1. Magnetite and melted rims on the particles indicate that these were solid, irregularly shaped grains during atmospheric entry and that their igneous portions thus did not form as a result of entry heating.
2. Allowing for changes during atmospheric entry (e.g., formation of vesicles), the mineralogies, textures, and compositions of the igneous objects strongly resemble those of chondrules. In particular, the distribution of mineral assemblages into reduced, Mg-silicate-dominated, oxidized Fe-bearing silicate-dominated, and radiating pyroxene objects is similar to that of chondrules.

3. Allowing for changes during atmospheric entry (e.g., Fe enrichment of mesostasis), the mineralogies, textures, and compositions of the fine-grained matrices and igneous objects in the composite particles strongly resemble those of the majority of fgMM and cgMM, implying that these particle types can be derived from the same set of primitive asteroidal parent bodies. The fine-grained matrix of the composite particles and fgMMs resembles the fine-grained matrix of CM2, CR2, and CI1 chondrites.
4. The composite particles suggest that igneous objects in MMs are small fragments (<50 μm) of igneous objects surrounded by fine-grained matrix and are thus similar to chondrule fragments commonly found in the chondrites.
5. The shapes of chondrules and their fragmentation during shock events suggest that dust particles derived from chondrules are unlikely to have smooth, curved surfaces or to preserve adjacent fine-grained matrices. In agreement with observation, smooth surfaces are most likely to be found on fragments of radiating pyroxene chondrules.

Alternative Explanations

Identifying a source other than chondrules for the igneous objects reported here is problematic. The chondritic mineral assemblages (i.e., olivine, low-Ca pyroxene and lesser amounts of feldspar/glass) and pyroxene minor element abundance suggest these are not samples of differentiated asteroids. They do not, however, preclude an origin from a primitive achondritic source. Grain sizes within the reported igneous objects are much smaller than those found in primitive achondrites and are difficult to reconcile with slow cooling. Similarly, although igneous clasts have been recognized in meteorites that have appropriate grain sizes, it is unclear whether many of these are derived as fragments of large 'megachondrules.' Certain 'chemically fractionated' igneous clasts, which contain phases such as cristobalite and nepheline and have trace-element abundances suggesting crystal-liquid fractionation (Bridges et al. 1997), can be dismissed as sources.

Impact melts provide one possible broadly chondritic source for igneous textured material within asteroidal parent bodies other than chondrules and are found in chondrites as veins, dykes, and clasts. Although they do have chondritic mineral assemblages similar to the observed igneous objects, impact melts are frequently glass-rich or finer-grained polymineralic materials and often contain abundant metal-sulfide droplets and so differ in texture from the observed particles. Impact melts also frequently contain angular unmelted clasts with evidence for shock such as equigranular, recrystallized textures or opaque shock veins consisting of numerous small metal blebs, none of which have been observed in the current study (e.g., Stoeffler et al. 1991). Shocked carbonaceous chondrites are also exceedingly rare (e.g., Scott et al. 1992).

The igneous objects in the reported MMs have chondritic mineralogies and thus are demonstrably not from a differentiated achondritic source. They could, however, be derived from igneous bodies larger than chondrules that have experienced little igneous fractionation or from impact melts. However, considering that most igneous clasts in the chondrites could have been derived as fragments of macrochondrules and that shock features have yet to be recognized in MMs, the most likely source for the reported composite and cgMMs is chondrules.

Implications

In the discussion above it is argued that: 1) igneous objects in composite MMs are probably fragments of chondrules, 2) fine-grained matrix in composite MMs is mineralogically, texturally, and chemically similar to fgMMs, and 3) igneous objects in composite MMs are similar to cgMMs, tentatively suggesting that many of these particles may likewise be fragments of chondrules.

The most important implication from the composite MMs is that at least a proportion of cgMMs can be derived from the same parent asteroids as fgMMs. Furthermore, the nature of fgMMs and cgMMs suggests that these parent bodies have affinities to CM/CR-chondrites and include both fine-grained matrix and chondrules. Micrometeorites are therefore not derived solely from unique, chondrule-free sources as previously suggested by Engrand et al. (1998).

Previous studies of the dynamics of asteroidal dust transport have suggested that micrometeoroids received at the Earth's surface are dominated by particles derived from low inclination, low eccentricity asteroidal dust bands that are associated with specific asteroidal families. Kortenkamp et al. (1998) suggested that the Koronis and Themis families dominate the micrometeoroid flux, while Nesvorny et al. (2003) identify Veritas, Koronis, and Themis families as the most important sources. The implication that cgMMs and fgMMs can be derived from the same set of asteroidal parent bodies would appear at face value to support these suggestions. The current research, however, implies only that a proportion of cgMMs may be derived from the carbonaceous chondrite-like parent bodies of fgMMs. These parent bodies are likely to be C-type asteroids, which are the most abundant asteroid type in the main belt.

Shock recovery experiments on carbonaceous chondrites have suggested that C-type asteroids with hydrous matrices may preferentially disaggregate due to dehydration during impact events and could dominate dust production in the main belt (Tomeoka et al. 2003). In contrast, the observation that anhydrous asteroid families, such as the S-type Koronis asteroids, are associated with significant dust bands (e.g., Nesvorny et al. 2003) suggests that a significant proportion of dust is produced by other types of asteroid.

A substantial fraction of cgMMs could therefore prove to be derived from other igneous sources that might be chondrule-dominated asteroids similar to the parent bodies of ordinary chondrites, at least in their overall chondrule abundances. The current research, however, has not established the genetic link between the majority of cgMMs and chondrules, only that RP cgMMs with smooth, curved surfaces and composite MMs are likely to represent samples derived from chondrules. Evaluating the overall parent body associations of MMs is beyond the scope of this work, as it requires a detailed comparison of cgMMs in general with chondrules. However, the presence of chondrules among MMs reported here does imply that their parent bodies are likely to be asteroids rather than comets, since current models suggest that cometary materials will be chondrule-free.

CONCLUSIONS

The composite MMs, comprised of fine-grained matrix materials and coarse-grained igneous objects, strongly imply that chondrule fragments are present among MM collections. These observations also suggest that many cgMMs may likewise be fragments of chondrules and that cgMMs and fgMMs can be derived from different components of the same parent asteroids.

Acknowledgments–The reviewers Ralph Harvey and Cecile Engrand are thanked for their useful comments.

Editorial Handling—Dr. Edward Scott

REFERENCES

Brearley A. J. and Jones R. H. 1998. Chondritic meteorites. In *Planetary materials*, edited by Papike J. J. Washington, D. C.: Mineralogical Society of America. pp. 1–191.

Bridges J. C. and Hutchison R. 1997. A survey of clasts and large chondrules in ordinary chondrites. *Meteoritics* 32:389–392.

Engrand C., Deloule E., Robert F., Maurette M., and Kurat G. 1999. Extraterrestrial water in micrometeorites and cosmic spherules from Antarctica: An ion microprobe study. *Meteoritics & Planetary Science* 34:773–786.

Engrand C. and Maurette M. 1998. Carbonaceous micrometeorites from Antarctica. *Meteoritics & Planetary Science* 33:565–580.

Ernstson K., Rampino M. R., and Hiltl M. 2001. Cratering of cobbles in Triassic Buntsandstein conglomerates in NE Spain: Shock deformation of in situ deposits in the vicinity of large impacts. *Geology* 29:11–14.

Genge M. J. 2002. Hydrated chondrules among micrometeorites (abstract). *Meteoritics & Planetary Science* 37:A51.

Genge M. J. 2004. Igneous rims on micrometeorites and the sizes of chondrules in main belt asteroids. (abstract #1102). 35th Lunar and Planetary Science Conference. CD-ROM.

Genge M. J. and Grady M. M. 1999. The fusion crusts of stony meteorites: Implications for atmospheric reprocessing of extraterrestrial materials. *Meteoritics & Planetary Science* 34: 341–356.

Genge M. J. and Grady M. M. 2002. The distribution of asteroids: Evidence from Antarctic micrometeorites (abstract #1010). 33rd Lunar and Planetary Science Conference. CD-ROM.

Genge M. J., Bradley J. P., Engrand C., Gounelle M., Harvery R. P., and Grady M. M. 2001. The petrology of fine-grained micrometeorites: Evidence for the diversity of primitive asteroids (abstract #1546). 32rd Lunar and Planetary Science Conference. CD-ROM.

Genge M. J., Grady M. M., and Hutchison R. 1997. The textures and compositions of fine-grained Antarctic micrometeorites: Implications for comparisons with meteorites. *Geochimica et Cosmochimica Acta* 61:5149–5162.

Greshake A., Kloeck W., Arndt P., Maetz M., Flynn G. J., Bajt S., and Bischoff A. 1998. Heating experiments simulating atmospheric entry heating of micrometeorites: Clues to their parent body sources. *Meteoritics & Planetary Science* 33:267–290.

Grossman J. N., Rubin A. E., Nagahara H., and King E. A. 1988. Properties of chondrules. In *Meteorites and the early solar system*, edited by Kerridge J. F. and Matthews M. S. Tucson, Arizona: The University of Arizona Press. pp. 619–659.

Klock W., Thomas K. L., McKay D. S., and Palme H. 1992. Unusual olivine and pyroxene composition in interplanetary dust and unequilibrated ordinary chondrites. *Nature* 339:126–128.

Kortenkamp S. J. and Dermott S. F. 1998. Accretion of interplanetary dust particles by the Earth. *Icarus* 135:469–495.

Nesvorny D., Bottke W. F., Levison H. F. and Dones L. 2003. Recent origin of the solar system dust bands. *The Astrophysical Journal* 591:486–497.

Kurat G., Hoppe P., and Engrand C. 1996. A chondrule micrometeorite from Antarctica with vapor-fractionated trace-element abundances (abstract). *Meteoritics & Planetary Science* 31:A75.

Kurat G., Koerberl C., Presper T., Brandstätter F., and Maurette M. 1994. Petrology and geochemistry of Antarctic micrometeorites. *Geochimica et Cosmochimica Acta* 58:3879–3904.

Maurette M., Olinger C., Christophe Michel-Levy M., Kurat G., Pourchet M., Brandstätter F., and Bourot-Denise M. 1991. A collection of diverse micrometeorites recovered from 100 tonnes of Antarctic blue ice. *Nature* 351:44–47.

Melosh H. J. 1996. *Impact cratering: A geologic process*. New York: Oxford University Press. 245 p.

Nakamura T., Noguchi T., Yada T., Nakamuta Y., and Takaoka N. 2001. Bulk mineralogy of individual micrometeorites determined by X-ray diffraction analysis and transmission electron microscopy. *Geochimica et Cosmochimica Acta* 65: 4385–4397.

Noguchi T., Nakamura T., and Nozaki W. 2002. Mineralogy of phyllosilicate-rich micrometeorites and comparison with Tagish Lake and Sayama meteorites. *Earth and Planetary Science Letters* 202:229–246.

Stoeffler D., Keil K., and Scott E. R. D. 1991. Shock metamorphism of ordinary chondrites. *Geochimica et Cosmochimica Acta* 55: 3845–3867.

Scott E. R. D., Keil K., and Stoeffler D. 1992. Shock metamorphism of carbonaceous chondrites. *Geochimica et Cosmochimica Acta* 56:4281–4293.

Taylor S. and Brownlee D. E. 1991. Cosmic spherules in the geological record. *Meteoritics* 26:203–211.

Taylor S., Lever J. H., and Harvey R. P. 2000. Numbers, types, and compositions of an unbiased collection of cosmic spherules. *Meteoritics & Planetary Science* 35:651–666.

Tomeoka K. and Buseck P. R. 1988. Matrix mineralogy of the Orgueil CI chondrite. *Geochimica et Cosmochimica Acta* 52: 1627–1640.

Tomeoka K., Kiriyama K., Nakamura K., Yamahana Y., and Toshimori S. 2003. Interplanetary dust from the explosive

dispersal of hydrated asteroids by impacts. *Nature* 423:60–62.
Toppani A., Libourel G., Engrand C., and Maurette M. 2001. Experimental simulation of atmospheric entry of micrometeorites. *Meteoritics & Planetary Science* 36:1377–1396.
Toppani A. and Libourel G. 2003. Factors controlling compositions of cosmic spinels: Application to atmospheric entry conditions of meteoritic materials. *Geochimica et Cosmochimica Acta* 67: 4621–4638.